String Gauge Unification and Infra-red Fixed Points in MSSM+X Models

B. C. Allanach[1] and S. F. King[2]

1. Rutherford Appleton Laboratory, Chilton, Didcot, OX11 0QX, U.K.
2. Physics Department, University of Southampton, Southampton, SO17 1BJ, U.K.

Abstract

In order to achieve gauge unification at the string scale $M_X \sim 5 \times 10^{17}$ GeV in the minimal supersymmetric standard model (MSSM) it is necessary to add extra gauge non-singlet representations at an intermediate scale $M_I < M_X$, leading to a class of models which we refer to as MSSM+X models. We perform a detailed analysis of a large class of MSSM+X models and find that the number of (3,1) representations added must be greater than the total of the number of (3,2) and (1,2) representations. Predictions of M_I, M_X and $\alpha(M_X)$ are obtained for models with up to 5 extra vector representations than the MSSM. Upper bounds on the U(1) string gauge normalisation k_1 and the sum of the squares of the hypercharge assignments of the extra matter are also obtained for the models. We also study the infra-red fixed point behaviour of the top quark Yukawa coupling in a large class of MSSM+X models and find that the low energy MSSM quasi-fixed point prediction of the top quark mass is more likely to be realised in these theories than in the MSSM. In other words the top quark tends to be heavier in MSSM+X models than in the MSSM. The implementation of a U(1)$_X$ family symmetry into MSSM+X models to account for the Standard Model fermion masses is discussed and a particular viable model is presented.

1 Introduction

The unification of the gauge couplings in supersymmetric grand unified theories
(SUSY GUTs) at a scale $M_{GUT} \sim 10^{16}$ GeV [1] is often regarded as a triumph of
the MSSM. Proponents of SUSY GUTs emphasise that such unification leads to a
prediction of $\sin^2 \theta_W$ at the 1% level, and the fact that the strong coupling $\alpha_s(M_Z)$
tends to come out on the large side is accounted for by threshold effects at the GUT
scale which could in principle lower α_s to any desired value in the experimental range.
However there are well known potential threats to SUSY GUTs arising from exper-
imental proton decay constraints on the one hand and theoretical doublet-triplet
splitting naturalness problems on the other. These two potential threats can both be
kept at bay at the expense of adding several large Higgs representations with carefully
chosen couplings. A further challenge to SUSY GUTs is the question of Yukawa ma-
trices, which again requires large Higgs representations. All these questions must and
can be addressed simultaneously, and there do exist realistic models in the literature
[2].

With the advent of string theory there is a different possibility for unification:
string gauge unification in which the gauge couplings are related to each other at the
string scale M_X [3]. String theories give the relation [4]

$$M_X = 5.3 \times 10^{17} g_X \text{ GeV},\qquad(1)$$

which is independent of the Kac-Moody level, where g_X is the unified gauge coupling
at the string scale M_X. In this framework it is not necessary to unify the couplings
into a SUSY GUT group, although it is possible to envisage a scenario in which a
SUSY GUT can be "derived" from the string [5, 6]. Such string derivations must yield
the desired large Higgs representations with the precise couplings required to avoid
proton decay, obtain doublet-triplet splitting, and yield realistic Yukawa matrices.
This is a technical feat which has not yet fully been accomplished, although there
has been some recent progress in this direction [6]. The existence of adjoint Higgs
representations requires the use of Kac-Moody level 2 Virasaro algebras or higher,
and while it is not impossible that Nature uses these higher levels, the simpler string
models are based on level 1 algebras. These are the so-called string inspired models
in which simple GUTs such as $SU(5)$, $SO(10)$ and so on are abandoned, and instead
the gauge couplings are unified at the string scale.

The simplest possible string-motivated model is clearly the minimal supersymmet-
ric standard model (MSSM). In this picture the MSSM (and nothing else) persists
right up to the string scale M_X. Naively such theories do not appear to be viable since
we know that the gauge couplings cross at $\sim 10^{16}$ GeV, and will have significantly
diverged at the string scale $\sim 5 \times 10^{17}$ GeV. However the situation is in fact not so
clear cut since the $U(1)_Y$ hypercharge gauge coupling has an undetermined normal-
isation factor $k_1 \geq 1$ (where for example $k_1 = 5/3$ is the usual GUT normalisation)
which may be set to be a phenomenologically desired value [7] by the choice of a
particular string model. However the simplest string theories (e.g. heterotic string
with any standard compactification) predict equal gauge couplings for the other two

observable sector gauge groups $g_2 = g_3$ at the string scale M_X, which would require a rather large correction in order to account for $\alpha_s(m_Z)$ [4, 8]. In fact, a recent analysis [9] concludes that string threshold effects are insufficient by themselves to resolve the experimental discrepancy. The analysis also concludes that light SUSY thresholds and two loop corrections cannot resolve the problem, even when acting together. In order to allow the gauge couplings to unify at the string scale it has been suggested [10] that additional exotic matter should be added to the MSSM at some intermediate scale or scales $M_I < M_X$, leading to a class of models which we shall refer to as MSSM+X models.

The purpose of the present paper is twofold. Firstly we shall perform a general unification analysis of a particular class of MSSM+X model. Then we shall study the infra-red fixed point properties of such models, focusing in particular on the top quark mass prediction. A detailed unification analysis of MSSM+X models has also been performed by Martin and Ramond (MR) [11]. MR considered the case of one or multiple intermediate thresholds, where the intermediate matter was contained in incomplete vector-like representations of E_6, either from chiral or vector supermultiplets. Gauge extensions at the intermediate scale were also considered [11]. The present unification analysis differs from the MR analysis in a number of ways as follows. Unlike MR, we shall consider arbitrary numbers of chiral superfields in low-dimensional vector representations, without any reference to an underlying E_6 model. Furthermore, unlike ref.[11], we shall not assume a GUT-type normalisation of the hypercharge generator but instead allow the possibility of different normalisations. Thus our analysis of string gauge unification is complementary to that of MR. Turning to our infra-red fixed point analysis of MSSM+X models, which was not considered at all by MR, we shall focus attention on the infra-red fixed point and quasi-fixed point of the top quark Yukawa coupling within the above class of MSSM+X models using similar techniques to those proposed for the MSSM and GUTs [12, 13, 14]. The main result is that the top quark mass tends to be heavier than in the MSSM, and closer to its quasi-fixed point in these models. Finally we speculate on the origin of Yukawa matrices with texture zeroes and small non-zero couplings within the MSSM+X framework, using the idea of a $U(1)$ gauged flavour symmetry and multiple Higgs doublets at the intermediate scale, similar to the proposal of Ibanez and Ross [15].

The layout of the rest of the paper is as follows. In section 2 we shall discuss string gauge unification of MSSM+X models, while in section 3 we shall consider the infra-red stable fixed point of the top quark Yukawa coupling in these models, and compare our results to those of the MSSM. In section 4 we shall briefly discuss the possibilities of obtaining realistic Yukawa matrices in this framework, identifying the intermediate matter with multiple Higgs doublets which, together with a $U(1)$ gauged flavour symmetry, may be used to generate realistic textures. Section 5 concludes the paper.

2   String Gauge Unification in MSSM+X Models

In this section we shall define the class of MSSM+X models under consideration and discuss our calculational procedures and the resulting predictions arising from string gauge unification in these models. Although there is inevitably some overlap in this section with ref.[11], we include our analysis in detail since as discussed above, our starting point is somewhat different. Furthermore the string scale, the intermediate scale and the string coupling will all be iteratively determined in our approach, leading to predictions for these quantities within particular models. Finally these results will be necessary for the discussion of the infra-red fixed points in the next section.

We shall impose string gauge unification subject to the following restrictions and assumptions: it is assumed that the gauge symmetry of the vacuum between the SUSY breaking scale M_{SUSY} and the string scale is SU(3)⊗SU(2)$_L$⊗U(1)$_Y$ and that the string theory is one of Kac-Moody level 1. The last assumption allows us to restrict the gauge representations since Kac-Moody level 1 strings only allow fundamental representations of the gauge group for the matter representations. Thus, the only possible extra matter representations we may add to the theory below M_X are (3,1), (1,2) and (3,2)[1] representations in (SU(3),SU(2)$_L$) space. The constraint of anomaly cancellation leads us to only add each of these representations to the MSSM in complete vector representations. We also assume for predictivity that the extra matter lies approximately at one mass scale $\sim M_I$. While this strong assumption is exact for 1 extra vector representation, it may be deemed increasingly unlikely for models in which more representations that are added.

The above restrictions are enough to give a predictive scheme that covers a large class of models. The origin of the magnitude of M_I or the quantum number assignments of the extra matter are dependent on the precise model of the string theory and so we do not consider these points in detail here. Possibilities for the generation of this scale include string-type non-renormalisable operators [9, 17] or operators generated by some hidden sector dynamics [18].

We define the number of vector (3,1) representations to be a, the number of vector (1,2) representations to be b, and the number of vector (3,2) representations to be c, where the vector representation corresponding to $(3,1)$ is $((\bar{3},1) \oplus (3,1))$ and so on for the other representations. We assume that each vector representation has an explicit mass M_I so that the effect of the extra vector representations is felt in the renormalisation scale region between M_I and M_X. Below M_I, the extra matter is integrated out of the effective field theory which then becomes the MSSM. The beta functions of the gauge couplings are defined by

$$16\pi^2 \frac{\partial g_i^2}{\partial t} = -b_i g_i^4, \tag{2}$$

where $t = \ln \mu_0^2/\mu^2$, g_i is the ith gauge coupling and μ_o, μ are the initial (high) and

---

[1]And other representations with either the 2 and or the 3 conjugated. This point makes no difference to our analysis.

final (low) $\overline{MS}$ renormalisation scales respectively. The beta functions of the effective theory between M_X and M_I are

$$b_i = \left(\left[11 + G_t \right] / k_1, \left[1 + b + 3c \right], \left[-3 + a + 2c \right] \right) \tag{3}$$

where k_1 is the string normalisation of the $U(1)_Y$ gauge coupling defined by

$$\alpha_1^{string} = k_1 \alpha_Y^{SM}, \tag{4}$$

α_Y^{SM} being the hypercharge gauge coupling in the standard model normalisation. A particular example $k_1 = 5/3$ yields the standard GUT normalisation

$$\alpha_1^{GUT} = (5/3) \alpha_Y^{SM}. \tag{5}$$

We have also used $G_t \equiv \Sigma_i (Y_i/2)^2$ where i runs over all of the superfields additional to the MSSM with Standard Model hypercharges $Y_i/2$.

In order to make the calculation as general as possible, model dependent factors such as string threshold corrections are not included. Given this substantial approximation, it is sufficient to use first order perturbation theory, a degenerate SUSY spectrum with mass M_{SUSY} and the step function approximation for mass thresholds in the renormalisation group (RG) equations. Using these approximations we obtain

$$\alpha_1(M_X)^{-1} = \frac{5}{3k_1} \left(\alpha_1(M_Z)^{-1} + \frac{53}{30\pi} \ln M_Z + \frac{17}{60\pi} \ln m_t + \frac{5}{4\pi} \ln M_{SUSY} + \right.$$
$$\left. \frac{3}{10\pi} G_t \ln M_I - \frac{3}{10\pi} (11 + G_t) \ln M_X \right) \tag{6}$$

$$\alpha_2(M_X)^{-1} = \alpha_2(M_Z)^{-1} - \frac{25}{12\pi} \ln M_Z + \frac{1}{2\pi} \ln m_t + \frac{25}{12\pi} \ln M_{SUSY} +$$
$$\frac{1}{2\pi} p \ln M_I - \frac{1}{2\pi} (1 + p) \ln M_X \tag{7}$$

$$\alpha_3(M_X)^{-1} = \alpha_3(M_Z)^{-1} - \frac{23}{6\pi} \ln M_Z + \frac{1}{3\pi} \ln m_t + \frac{2}{\pi} \ln M_{SUSY} +$$
$$\frac{1}{2\pi} (a + 2c) \ln M_I + \frac{1}{2\pi} (3 - a - 2c) \ln M_X \tag{8}$$

where the $\alpha_i(M_X) \equiv \alpha_i^{string}(M_X)$ are all in the string normalisation and $\alpha_1(M_Z)^{-1} \equiv \alpha_1^{GUT}(M_Z)^{-1} = 58.89$ is in the GUT normalisation. We have defined the positive integer $p = b + 3c$, which counts the number of additional $SU(2)_L$ doublets. Note that all of the mass scales referred to in this paper are $\overline{MS}$ running masses, except pole masses which are denoted with a superscript $phys$. For example, to first order, the top quark pole mass is related to its running mass by

$$m_t^{phys} = m_t \left[1 + 4\alpha_s \frac{m_t}{3\pi} \right]. \tag{9}$$

The normalisation k_1 is very model dependent, the most general constraint upon it is that it must be rational and greater than or equal to one [7, 19]. We therefore

4

regard it as a free parameter and so have one less prediction, that of $\sin^2 \theta_W$, compared to SUSY GUTs. Eq.1 partly compensates for this by a prediction of the string scale M_X in terms of any of the gauge couplings. Once M_X is determined, the left hand sides of Eqs.7,8 may be equated to yield a prediction for the intermediate scale

$$\ln \frac{M_I}{M_X} = \frac{1}{n} \left[4 \ln M_X - \left(2\pi(\alpha_2(M_Z)^{-1} - \alpha_3(M_Z)^{-1}) + \frac{7}{2} \ln M_Z + \frac{1}{3} \ln m_t + \frac{1}{6} \ln M_{SUSY} \right) \right], \tag{10}$$

where the integer n is defined by $n \equiv b + c - a$. Eq.10 allows us to get a bound on n by applying the constraint $M_I < M_X$. Using the input parameters $\alpha_2(M_Z)^{-1} = 29.75$, $\alpha_3(M_Z) = 0.112 - 0.122$, $m_t^{phys} = 152 - 196$ GeV^2, $M_X = 3 - 5 \times 10^{17}$ GeV and $M_{SUSY} = 200 - 1000$ GeV, we obtain that the quantity within the square brackets on the right hand side of Eq.10 is always positive and hence $n < 0$, or

$$a > b + c. \tag{11}$$

All of the possible MSSM+X models satisfying Eq.11 with up to 5 vector representations added are displayed in Table 1. It is upon these simple examples that we shall focus our attention.

For the case of many extra gauge representations to the MSSM with mass $\sim M_I$, another bound may be placed upon a, b, c as follows. Eq.s 7,10,1 may be rearranged such that the ratio p/n may be expressed in terms of $\alpha_2(M_X)^{-1}$:

$$\frac{p}{n} = \frac{2\pi\alpha_2(M_X)^{-1} - \frac{1}{2} \ln \left(\frac{\alpha_2(M_X)^{-1}}{4\pi} \right) + \ln Z - 2\pi X}{4 \ln Z - 2 \ln \left(\frac{\alpha_2(M_X)^{-1}}{4\pi} \right) - Y}, \tag{12}$$

where we have defined

$$X \equiv \alpha_2(M_Z)^{-1} - \frac{25}{12\pi} \ln M_Z + \frac{25}{12\pi} \ln M_{SUSY} + \frac{1}{2\pi} \ln m_t$$

$$Y \equiv 2\pi \left(\alpha_2(M_Z)^{-1} - \alpha_3(M_Z)^{-1} \right) + \frac{7}{2} \ln M_Z + \frac{1}{3} \ln m_t + \frac{1}{6} \ln M_{SUSY}$$

$$Z = 5.3 \times 10^{17} \text{ GeV}.$$

The right hand side of Eq.12 is rather complicated but can be investigated numerically as a function of $\alpha_2(M_X)^{-1}$. We find that p/n has a minimum as a function of $\alpha_2(M_X)^{-1}$, albeit with a large uncertainty from $\alpha_3(M_Z)$. When the minimum of Eq.12 is determined numerically, we obtain the bound

$$p/n > K, \tag{13}$$

where $K = -11.0, -9.2, -8.0$ for $\alpha_S(M_Z) = 0.112, 0.117, 0.122$ respectively. Since n must be negative, and p is positive, the bound may be written as

$$p < |n||K|, \tag{14}$$

from which we see that the number of doublets p is bounded from above. This bound is not approached for the models in Table 1, but will be relevant when we come to consider the origin of the Yukawa matrices in section 4.

---

[2]The top quark mass measurement by the CDF collaboration [20].

Model	N	a	b	c	n	p
A	1	1	0	0	-1	0
B	2	2	0	0	-2	0
C	3	2	1	0	-1	1
D	3	2	0	1	-1	3
E	3	3	0	0	-3	0
F	4	3	1	0	-2	1
G	4	3	0	1	-2	3
H	4	4	0	0	-4	0
I	5	3	1	1	-1	4
J	5	3	2	0	-1	2
K	5	3	0	2	-1	6
L	5	4	1	0	-3	1
M	5	4	0	1	-3	3
N	5	5	0	0	-5	0
X	25	14	10	1	-3	13

Table 1: MSSM+X models with $N \leq 5$ additional chiral superfields in vector representations of the MSSM that satisfy Eq.11. The 7 columns detail the names and content of the models, where a, b, c are the number of chiral scalar fields in the vector rep.s $(3, 1), (1, 2), (3, 2)$, respectively, and $n = b + c - a$, $p = b + 3c$. The final row details a special model containing $N = 25$ additional superfields, which is introduced for the purposes of the discussion in section 4.
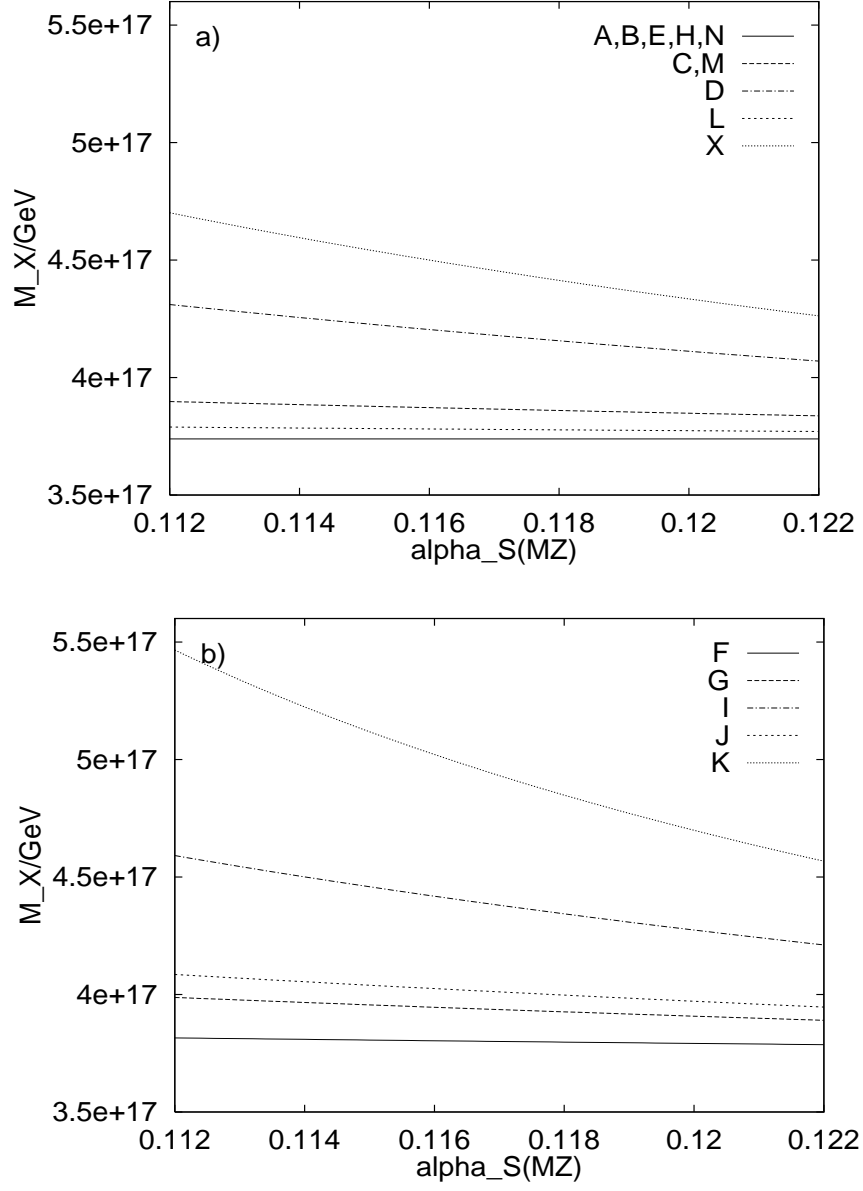
Figure 1: Prediction of the string scale M_X in the MSSM+X models for $M_{SUSY} = 500$ GeV, $m_t^{phys} = 174$ GeV and various $\alpha_S(M_Z)$. The key identifies the model by reference to Table 1.

To extract M_X in practice requires an iterative numerical procedure. First a scale $\Lambda \sim 5.10^{17}$ GeV is substituted for M_X in Eq.10 to give an M_I consistent with gauge unification at a scale Λ. This value of M_I is then substituted into Eq.7 to yield $\alpha(\Lambda)^{-1}$. Substituting $\alpha(\Lambda)$ into Eq.1 yields what string breaking scale M_X would correspond to this gauge coupling. This M_X is substituted for Λ and the whole process is repeated until $\Lambda = M_X$ is converged upon. If this procedure converges, we are left with numerical values of $M_I, M_X, \alpha_i(M_X)$ that are consistent with gauge unification in the model under study.

Fig.1 displays the values of M_X given by this procedure for the models outlined in Table 1. Central values of m_t, M_{SUSY} were picked and the results have negligible sensitivity upon m_t. Varying M_{SUSY} between 200 and 1000 GeV changes the M_X prediction by $\sim 0.1 \times 10^{17}$ GeV. As shown, the results are in general quite dependent upon the strong coupling constant $\alpha_S(M_Z)$ and so we have used this as the independent parameter in the plots. In Fig.2 the running of the gauge couplings in model K is compared to the running purely within the MSSM. At M_I, the effects of the extra representations are felt and $\alpha_{2,3}$ rise steeply with μ. The general tendency shown by Fig.1 is that M_X is higher for models which possess the most $SU(2)_L$ doublets (high p), and lower for models in which the number of $SU(3)$ triplets minus the number of $SU(2)_L$ doublets is great (more negative n). The class $p = 0$ when there are no added doublets for models A,B,E,H,N is a special class of cases in which there is no $\alpha_S(M_Z)$ dependence to 1 loop. Because there are no more $SU(2)$ representations than the MSSM, the running of α_2 is identical to the MSSM until the GUT scale M_G. This alone fixes $M_X, \alpha_i(M_X)$ in these cases, since for $p = 0$, Eq.1 and Eq.7 could be combined to give an equation with only one output: M_X for example. An example of this case is model A ($n = -1, p = 0$), which is examined in more detail in Fig.3. It is shown in the figure that when different initial values of $\alpha_S(M_Z)$ are taken, M_I conspires to give the same value of M_X (and therefore $\alpha_i(M_X)$).

Figs.5,6 show the predictions for M_I for each of the models $A, B, \ldots, N$. Varying M_{SUSY} between 200 and 1000 GeV makes a maximum difference to $\ln M_I$ of $\sim 2\%$ and the results (like all of the gauge unification predictions) are not very dependent on $m_t^{phys} = 152 - 196$ GeV. The results are dependent upon the value of n that is relevant for the model in question. This is because n counts the number of extra $SU(2)_L$ doublets minus the number of extra $SU(3)$ triplets in the model. This point is illustrated in Fig.4, where model A ($n = -1, p = 0$) is compared with model H ($n = -4, p = 0$). Models with $p = 0$ have $M_X, \alpha_i(M_X)$ fixed independent of n as stated previously and models with higher $-n$ have more positive slopes in the region $M_I < \mu < M_X$. Thus, to hit the same endpoint of $\mu = M_X, \alpha_i(\mu)$, the lower $-n$ models must have lower M_I in order to agree with the low energy gauge couplings.

The predictions of $\alpha_i(M_X)$ vary a lot depending upon how many $SU(2)_L$ doublets are present in the intermediate region $M_I < \mu < M_X$, as shown by Fig.7. Models with high values of p tend to have high $\alpha_i(M_X)$ because $b_{2,3}$ (and therefore the rates of change of the gauge couplings with respect to μ) are more positive, as Fig.2 shows. $\alpha_i(M_X)$ is approximately not dependent upon m_t and $M_{SUSY} = 200 - 1000$ GeV
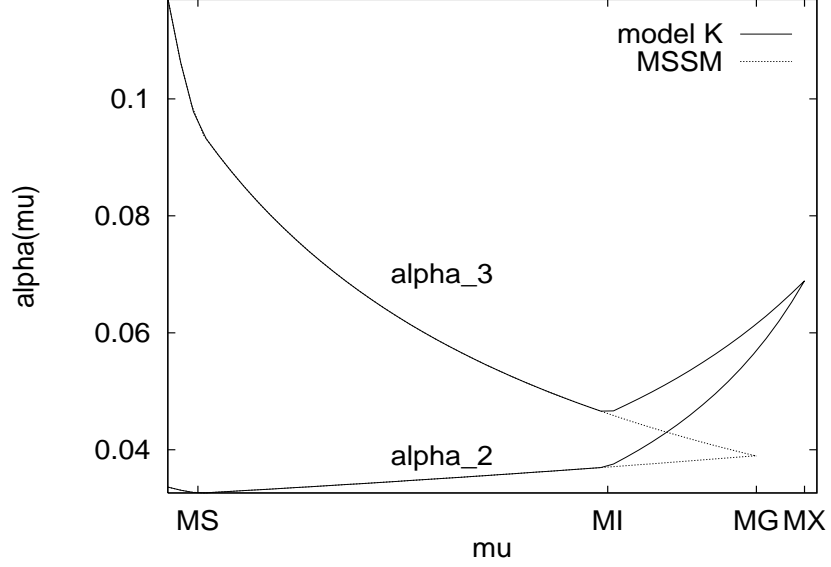
Figure 2: Comparison between model K and the MSSM of the running of the gauge coupling constants α_2, α_3. The running is between $\mu = M_Z$ and $\mu = M_X, M_G = 10^{16}$ GeV for $m_t^{phys} = 174$ GeV, $M_{SUSY} = 500$ GeV and $\alpha_S(M_Z) = 0.117$.
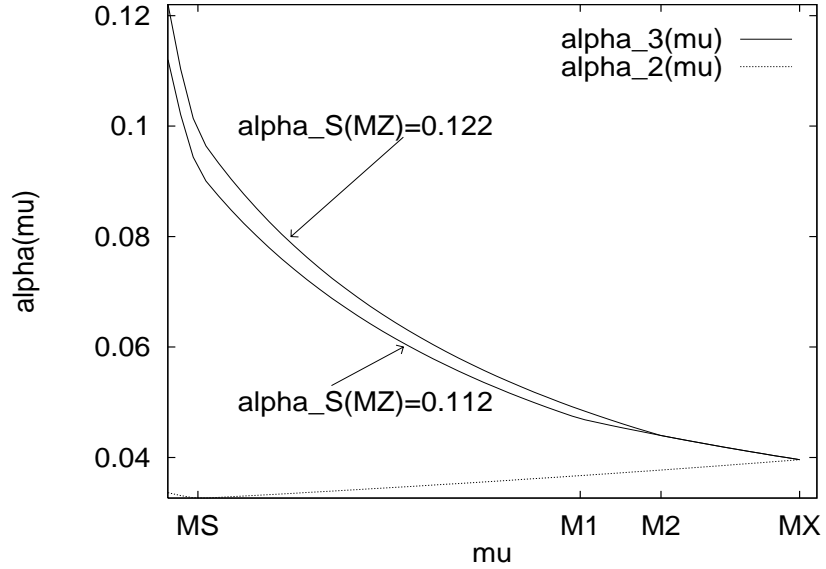

Figure 3: Running of the SU(3) and SU(2)$_L$ gauge coupling constants in model A between M_Z and M_X for $m_t^{phys} = 174$ GeV, $M_{SUSY} = 500$ GeV. $M_I \equiv M1, M2$ correspond to $\alpha_S(M_Z) = 0.112, 0.122$ respectively.
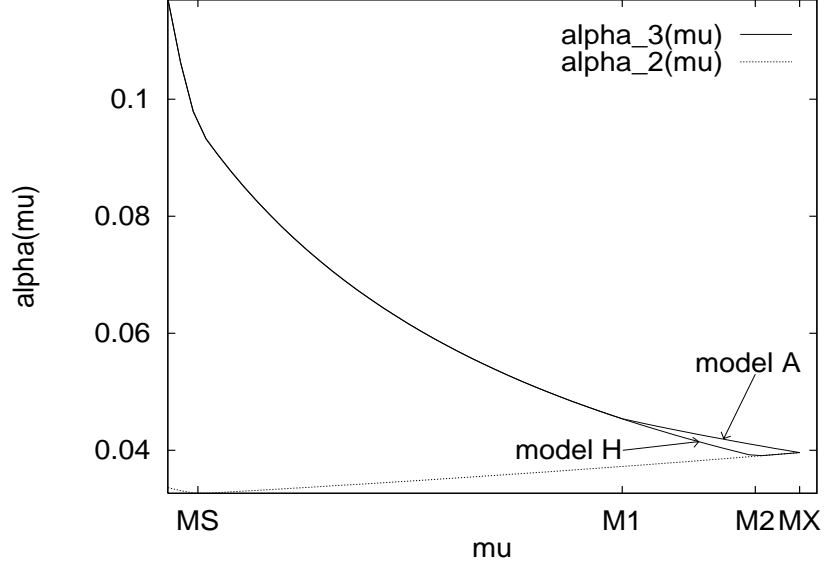
9

Figure 4: Comparison of the running of the gauge coupling constants in model A and model H. The running is between $\mu = M_Z$ and $\mu = M_X$ for $m_t^{phys} = 174$, GeV $M_{SUSY} = 500$ GeV and $\alpha_S(M_Z) = 0.117$. $M_I \equiv M1, M2$ correspond to models A,H respectively.
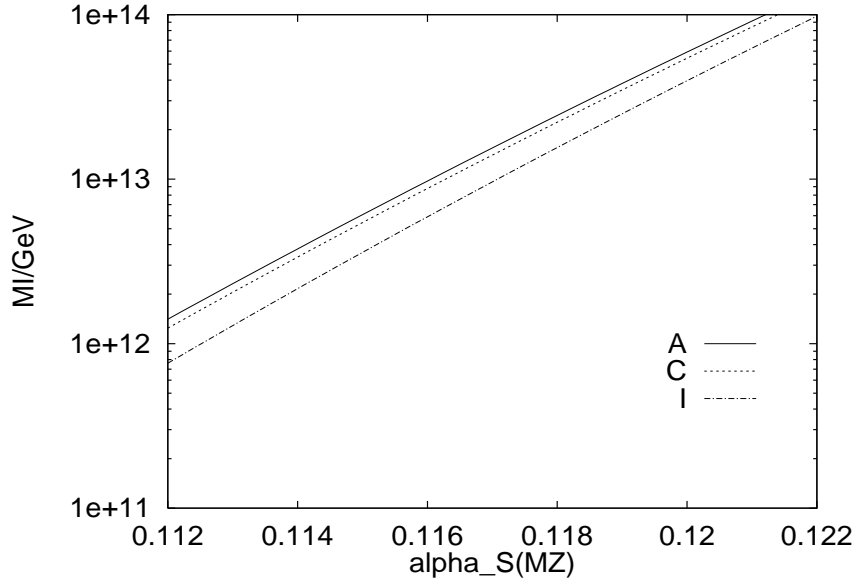

Figure 5: Prediction of the intermediate scale M_I in the MSSM+X models indicated in the key for $M_{SUSY} = 500$ GeV, $m_t^{phys} = 174$ GeV and various $\alpha_S(M_Z)$.
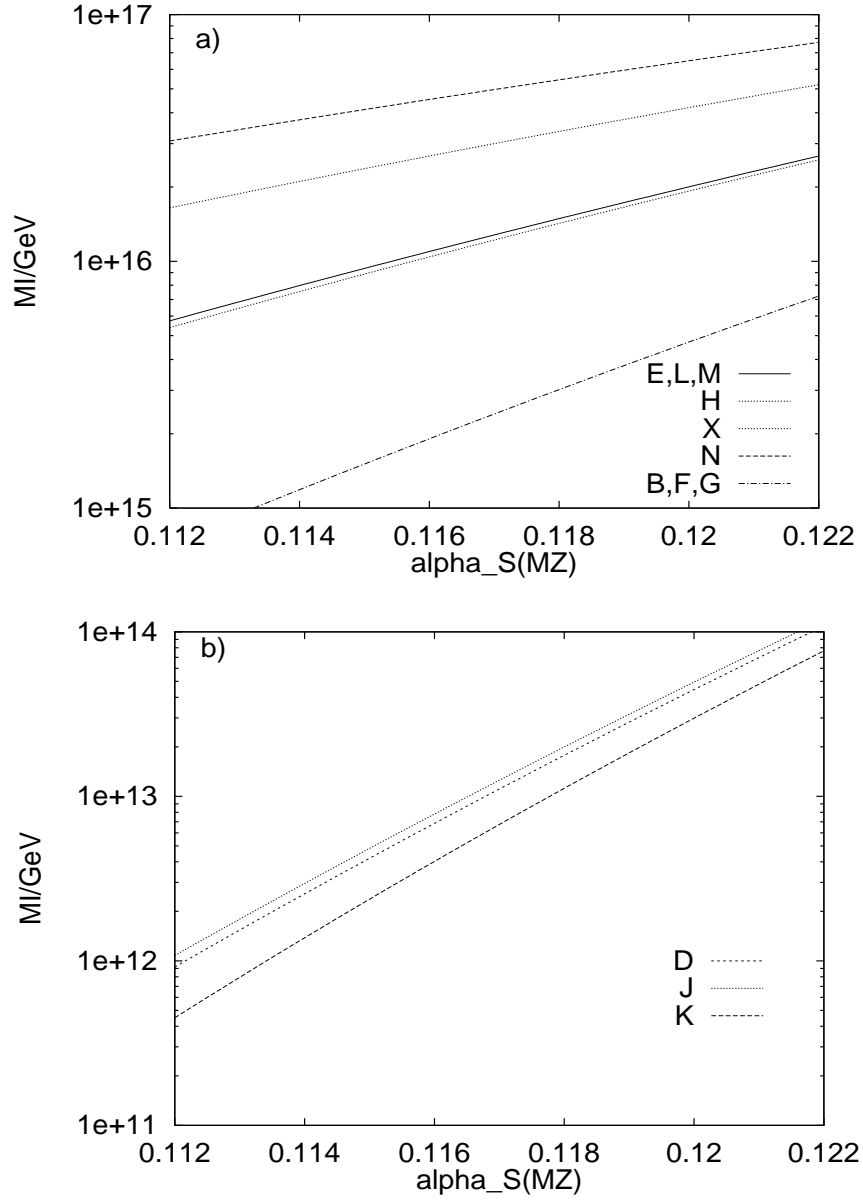
Figure 6: Prediction of the intermediate scale M_I in the MSSM+X models indicated in the key for $M_{SUSY} = 500$ GeV, $m_t^{phys} = 174$ GeV and various $\alpha_S(M_Z)$.
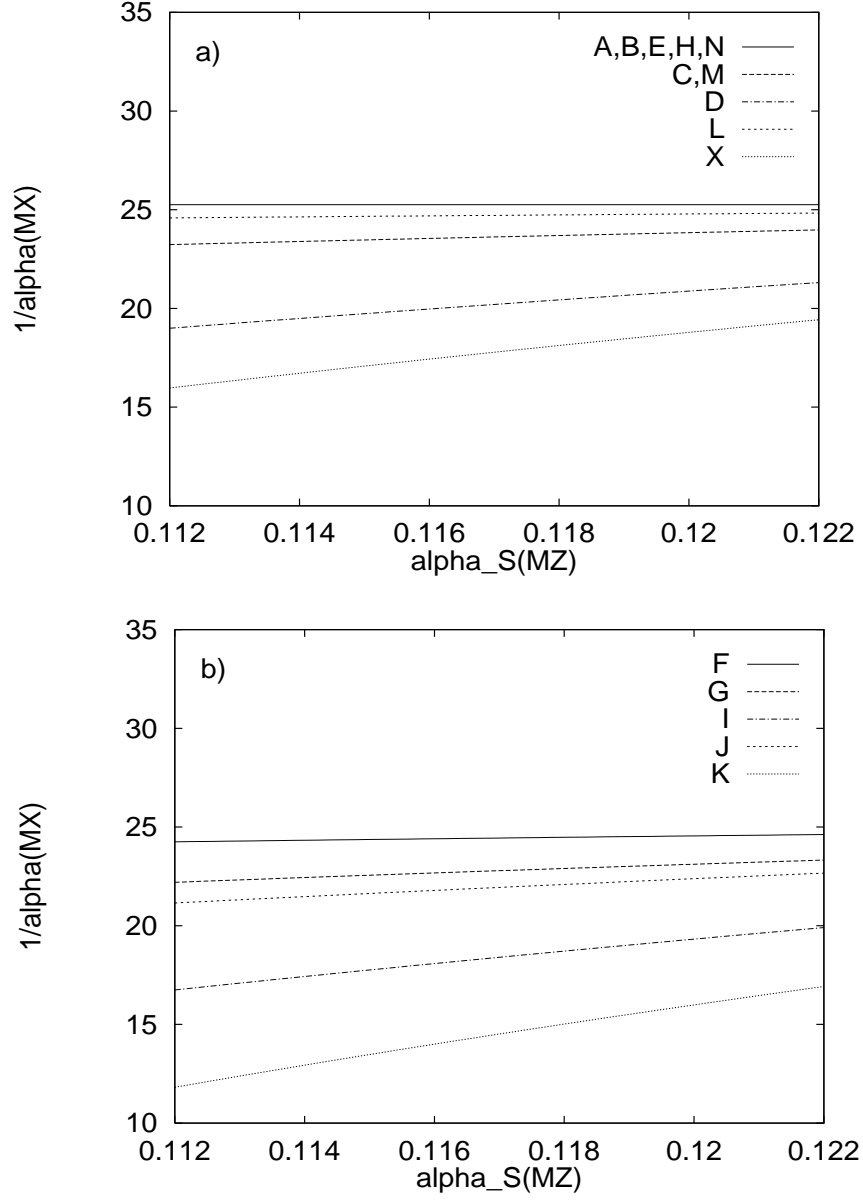
Figure 7: Prediction of the string gauge coupling $\alpha(M_X)^{-1}$ in the MSSM+X models for $M_{SUSY} = 500$ GeV, $m_t^{phys} = 174$ GeV and various $\alpha_S(M_Z)$. The key identifies the model by reference to Table 1.

$\alpha_S(M_Z)$	A	B	C	D	E	F	G	H	I	J	K	L	M	N
0.112	5.7	11	16.5	8	17	12	14	22	9	7	11	18	20	28
0.122	9.1	18	9.8	11	27	19	20	36	12	11	14	28	29	45

Table 2: Upper bounds on G_t for $M_{SUSY} = 200 - 1000$ GeV and $m_t^{phys} = 152 - 196$ GeV for the MSSM+X models in Table 1.

corresponds to a change in $\alpha_i(M_X)$ of $\sim 2\%$.

We may now extract some more information about the string theory from which the MSSM+X models must derive by examining the unification of the hypercharge gauge coupling. Setting the right hand sides of Eqs.6,7 equal yields an equation

$$k_1 = \frac{5}{3} \frac{2\pi\alpha_1(M_Z)^{-1} + \frac{53}{15}\ln M_Z + \frac{17}{30}\ln m_t + \frac{5}{2}\ln M_{SUSY} - \frac{3G_t}{5}\ln\left(\frac{M_X}{M_I}\right) - \frac{33}{5}\ln M_X}{2\pi\alpha_2(M_Z)^{-1} - \frac{25}{6}\ln M_Z + \ln m_t + \frac{25}{6}\ln M_{SUSY} + p\ln M_I - (1+p)\ln M_X}.$$

(15)

Eq.15 cannot be used to predict the string normalisation k_1 since G_t is arbitrary and unknown. However, an upper bound may be placed upon k_1 by noting that G_t is positive semi-definite. Setting $G_t = 0$ in Eq.15 therefore gives the maximum string normalisation upon the hypercharge assignments consistent with gauge unification at the string scale, and therefore placing that constraint upon the string theory that is supposed to reduce to the MSSM+X model as the low energy effective field theory limit. Fig.8 displays the upper bounds upon k_1 for the MSSM+X models A,B,...,N. Higher p and lower $-n$ corresponds to a higher upper bound, mostly because in these cases $\alpha_i(M_X)$ is large, as explained earlier. Again, the results are roughly independent of m_t and only depend on M_{SUSY} at the $\sim 2\%$ or less level. As an example, the only MSSM+X models studied here that are consistent with the GUT normalisation of $k_1 = 5/3$ are D,I,J,K,X. The bound $k_1 \geq 1$ [7] may be used in Eq.15 to place an upper bound upon G_t. As Table 2 shows, the maximum hypercharge assignments for the extra matter are large compared with typical hypercharges in the Standard Model. The numbers are so large that they are unlikely to be a strong constraint on a given string model (for the whole of the MSSM, $\sum_i(Y_i/2)^2 = 11$). Once k_1 is picked in the context of a particular string model, G_t is then fixed. As an example of what possible hypercharge normalisations may result, we focus on the particular example of model D, which is equivalent to the MSSM plus 2 right handed quark representations and one left handed quark representation at the scale $M_I \sim 10^{12-14}$ GeV. Assuming these superfields have the same Standard Model hypercharge assignments as Q_L, u_R, d_R respectively, we obtain $k_1 \sim 5/3$.
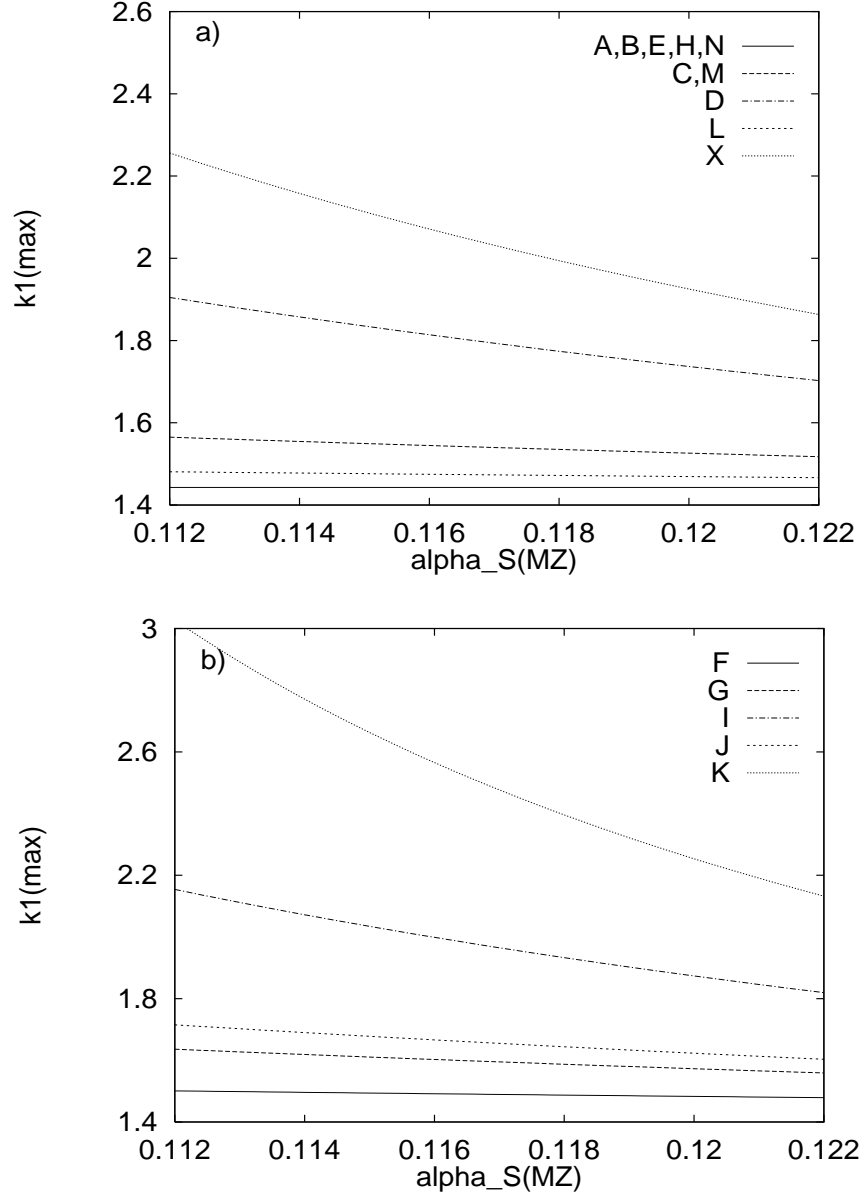
Figure 8: The maximum value of k_1 in the MSSM+X models for $M_{SUSY} = 500$ GeV, $m_t^{phys} = 174$ GeV and various $\alpha_S(M_Z)$. The key identifies the model by reference to Table 1.

3 Infra-red Fixed Points in MSSM+X Models

Lanzagorta and Ross [14] recently revisited the fixed point [12, 13] in the RGEs of the top quark Yukawa coupling and QCD gauge coupling in the framework of MSSM and SUSY GUT models. In this section we shall extend their analysis to the MSSM+X models considered in the previous section.

The effective superpotential of the MSSM+X models is assumed to be

$$W = h_t Q H_2 u^c - \mu H_1 H_2 + \ldots \tag{16}$$

where h_t is the top Yukawa coupling, Q, u^c refer to the third family left handed quark and right handed quark superfields and $H_{1,2}$ are the two Higgs doublet superfields. It has been assumed in Eq.16 that the ratio of Higgs vacuum expectation values (VEVs) $\tan \beta \equiv v_2/v_1$ is of order one and all small Yukawa couplings have been dropped. The terms due to the extra matter are assumed to be all of the forms $M_I(3,1).(\bar{3},1)$, $M_I(1,2).(1,\bar{2})$, $M_I(3,2).(\bar{3},\bar{2})$ where the group indices are traced over. Thus, these terms would give the extra matter a mass M_I but no extra parameters would enter the one loop top quark Yukawa coupling renormalisation group equation compared to the MSSM. Note that this could be a consequence of the extra matter having non-standard hypercharge assignments[19], so that an additional superfield could not couple to a MSSM superfield with opposite SU(3)⊗SU(2) quantum numbers in a hypercharge invariant way.

The RGE for the case of only one large Yukawa coupling is

$$\frac{\partial Y_t}{\partial t} = Y_t \left(\Sigma_i r_i \tilde{\alpha}_i - s Y_t \right), \tag{17}$$

where we have defined the parameters in the same notation as Lanzagorta and Ross [14] $\tilde{\alpha}_i \equiv g_i^2/16\pi^2$, $Y_t \equiv h_t^2/16\pi^2$. Dropping the electroweak gauge couplings, Eq.17 can be written as,

$$\frac{\partial R}{\partial t} = Y_t \left[(r_3 + b_3) - sR \right] \tag{18}$$

where the ratio of Yukawa to gauge coupling has been written as

$R = \left(\frac{Y_t}{\tilde{\alpha}_3} \right)$. For the MSSM, $r_3 = 16/3, b_3 = -3, s = 6$. Eq.18 has an infra-red stable fixed point given by

$$R^* = \left(\frac{Y_t}{\tilde{\alpha}_3} \right)^* = (r_3 + b_3)/s = 7/18. \tag{19}$$

as shown by Fig.9, where the asterisk denotes the fixed point. The figure shows that $(Y_t/\tilde{\alpha})$ at an arbitrary scale is attracted towards the fixed point as the energy scale is reduced. The low energy value of $R = (Y_t/\tilde{\alpha})$ is given by

$$R(t) = \frac{R^*}{1 + \Delta \left[\frac{R^*}{R(0)} - 1 \right]} \tag{20}$$
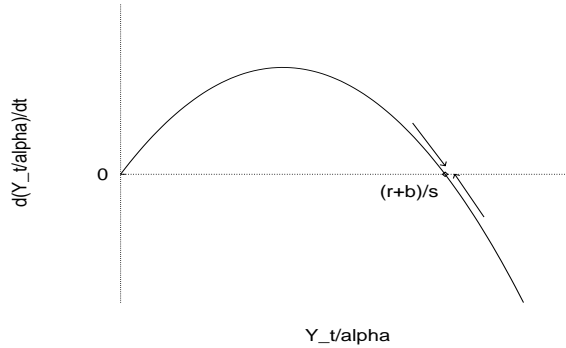
Figure 9: Infra red behaviour of $Y_t/\tilde{\alpha}$ in the case when the top Yukawa coupling is dominant. The arrows indicate the direction of flow for increasing t, i.e. in the direction of the infra-red direction. The point labeled $(r + b)/s$ is the fixed point.

where we have defined

$$\Delta = \left(\frac{\alpha_3(t)}{\alpha_3(0)} \right)^{B_3}, \tag{21}$$

$B_3 \equiv r_3/b_3 + 1$ and $t = \ln M_X^2/\mu^2$ where μ refers to the low energy scale and $t = 0$ corresponds to $\mu = M_{GUT}$.

There is no a priori reason why the high energy theory should select the boundary condition on the top quark Yukawa coupling to be at its fixed point. However Eq.20 shows that for arbitrary input value the fixed point value is always reached in the limit $t \to \infty$ since in this limit $\Delta \to 0$ (since $B_3 = -7/9$ and α_3 is asymptotically free). In practice Δ is finite ($\Delta \sim 0.5$ in the MSSM from the running between GUT and weak scales) and the low energy value of the top quark Yukawa coupling will be higher or lower than its fixed point value, depending on the whether the high energy input value of the coupling is higher or lower than its fixed point value. However it is well known that, for fixed t, there is a maximum low energy value of top quark Yukawa coupling corresponding to $Y_t(0) \to \infty$. In fact this maximum value is achieved to very good accuracy by finite but large input values which satisfy the condition

$$R(0) \gg R^* \tag{22}$$

which allows the simple approximate form of Eq.20

$$R(t) \approx \frac{R^*}{1 - \Delta} \equiv R^{QFP} \tag{23}$$

which is the well known quasi-fixed-point (QFP)[13]. It is worth emphasising that, given only that the condition in Eq.22 is met, Eq.23 gives an (approximate) determination of the low energy top quark Yukawa coupling which is quite insensitive to its high energy value. To be more specific, for any choice of input top Yukawa couplings $R(0) > R^*$ the low energy values of the top quark Yukawa couplings will be funneled

into a range between R^* and R^{QFP} where the distance between the FP and QFP is controlled by the quantity Δ defined in Eq.21. The smaller the quantity Δ, the closer will be the QFP to the FP, and the more accurate will be the determination of the low energy top Yukawa coupling.[3]

Lanzagorta and Ross [14] also considered the effect of various GUT theories above the scale $M_{GUT} \approx 10^{16}$ GeV. Just as the MSSM may be analysed in the range $M_{GUT} - M_{SUSY}$ so the SUSY GUT theory was analysed in the range $M_P - M_{GUT}$, using similar techniques. In SUSY GUT theories containing a large number of representations, asymptotic freedom may be lost and the gauge coupling can grow rapidly as it approaches M_P. It was argued that in such a case, the fixed point structure in the range $M_P - M_{GUT}$ may be more important than the MSSM fixed point [14]. It was subsequently argued that the effect of such a SUSY GUT would be to lead to a low energy top quark Yukawa coupling closer to its QFP value than the MSSM expectation [14].

The fixed point nature in the SUSY GUT in the region $M_P - M_{GUT}$ is seen from the following result, obtained by analogy with earlier results, for the top quark Yukawa coupling at the GUT scale,

$$R(M_{GUT}) = \frac{R^*_{GUT}}{1 + \Delta_{GUT} \left[\frac{R^*_{GUT}}{R(M_P)} - 1 \right]} \tag{24}$$

where above we have replaced t by its lower argument μ, in order to help keep track of which energy scale we are referring to, and defined

$$\Delta_{GUT} = \left(\frac{\alpha(M_{GUT})}{\alpha(M_P)} \right)^{B_{GUT}} \tag{25}$$

where $B_{GUT} \equiv r/b + 1$ for the GUT theory, and $\alpha(\mu)$ is the GUT gauge coupling at the scale μ, with $R = (Y_t/\tilde{\alpha})$. Clearly the QFP for the GUT theory is achieved when the following condition is met,

$$R(M_P) \gg R^*_{GUT} \tag{26}$$

which when satisfied leads to the approximate result

$$R(M_{GUT}) \approx \frac{R^*_{GUT}}{1 - \Delta_{GUT}} \equiv R^{QFP}_{GUT} \tag{27}$$

In the type of theories considered by Lanzagorta and Ross [14] (i.e. very non-asymptotically free GUT theories) they find that

$$R^*_{GUT} \gg R^*_{MSSM}, \tag{28}$$

---

[3]Parenthetically we note that the above analysis is not valid for the special case when $b_3 = 0$, so that Eq.17 decouples from the running of the gauge coupling. In this case, $Y^* = r\tilde{\alpha}/s$, with solution $Y(t) = \frac{Y^*}{\frac{Y^*}{Y(0)} e^{-r\alpha t} - e^{-r\alpha t} + 1}$ and the maximum distance from fixed point $\Delta = e^{-r\alpha t}$. Note that in a case where $b < 0$ and $r < -b$, $Y_t \to 0$ at low energy and has no infra-red fixed point since $\left(\frac{\alpha_3(t)}{\alpha(0)} \right)^{B_3} \to \infty$ as $t \to \infty$. This does not apply to any of the models examined in this paper.

The result in Eq.28 implies that the SUSY GUT is less likely to satisfy its QFP condition in Eq.26.[4] For SUSY GUTs with many added vector families, $\Delta_{GUT} \ll \Delta_{MSSM}$ implies that the GUT FP is realised more accurately at the GUT scale. The important question, however, is the effect of the combination of these two results on the low energy top quark Yukawa coupling; the effect is to drive it more closely to its MSSM QFP value as seen below.

In order to investigate the effect of the SUSY GUT theory on the low energy top Yukawa coupling, Lanzagorta and Ross first re-wrote Eq.24 as

$$x' = x\Delta_{GUT} + \frac{R^*_{MSSM}}{R^*_{GUT}}(1 - \Delta_{GUT}) \tag{29}$$

where

$$x' \equiv \frac{R^*_{MSSM}}{R(M_{GUT})}, \quad x \equiv \frac{R^*_{MSSM}}{R(M_P)} \tag{30}$$

The quantity x should not be confused with the quantity which gives the condition for the GUT QFP in Eq.26 which is

$$y \equiv \frac{R^*_{GUT}}{R(M_P)} \tag{31}$$

where $y \ll 1$ is the GUT QFP condition. The quantity x' is identified as the ratio $\frac{R^*}{R(0)}$ in Eq.20, which may consequently be written as,

$$R(M_{SUSY}) = \frac{R^*_{MSSM}}{1 + \Delta_{MSSM}[x' - 1]} \tag{32}$$

The combination of Eqs.29 and 32 give us all the information we need to decide the fate of the low energy top quark Yukawa coupling. The condition for the MSSM QFP is clearly just $x' \ll 1$, where x' is given in Eq.29. According to Eq.28 we have from Eq.29

$$x' \approx x\Delta_{GUT} \tag{33}$$

Since $\Delta_{GUT} < 1$ Eq.33 shows that a given value of x implies a smaller value of x'. Thus the effect of such SUSY GUTs is to make it more likely that the low energy top Yukawa coupling is at its MSSM QFP, as claimed [14].

We now turn to the question of the infra-red nature of MSSM+X models. [5] This approach to MSSM+X theories turns out to have many similarities to the case of SUSY GUTs considered above; for example in MSSM+X theories with a large number

---

[4]The SUSY GUT QFP condition is explicitly $Y_t(M_P) \gg \tilde{\alpha}(M_P)R^*_{GUT}$ where both R^*_{GUT} and $\tilde{\alpha}(M_P)$ are typically much larger than in the MSSM. This implies that $Y_t(M_P)$ would have to be *substantially* larger than its MSSM equivalent in order for the QFP to be relevant for the SUSY GUT theory, leading to the danger of perturbation theory breakdown for the top Yukawa coupling.

[5]In some superstring models, the top quark Yukawa coupling is predicted at the string scale. For example ref. [21] discusses such a mechanism, including the effects of intermediate matter. In order to remain as model independent as possible, in our present analysis we shall instead regard h_t to be unconstrained at M_X.

of exotic colour triplets, asymptotic freedom of QCD is lost above the intermediate scale. It would therefore be expected that in such MSSM+X models, the low energy top quark Yukawa coupling is more likely to be at its MSSM QFP, as in SUSY GUTs, and we find that this is indeed the case. The analytic results for the MSSM+X models may be more or less taken over immediately from the SUSY GUT results given above, by making the following obvious replacements in Eqs.24-33:

$$M_P \to M_X, \quad M_{GUT} \to M_I, \quad R_{GUT} \to R_X, \quad \Delta_{GUT} \to \Delta_X, \quad \alpha \to \alpha_3 \qquad (34)$$

Note that in the present case there is no fixed scale which separates the MSSM from the MSSM+X theory, since M_{GUT} has been replaced by the intermediate scale M_I which can range over several orders of magnitude. This implies that Δ_{MSSM} is no longer a fixed quantity, since it is given by,

$$\Delta'_{MSSM} = \left(\frac{\alpha(M_{SUSY})}{\alpha(M_I)} \right)^{B_3} \qquad (35)$$

and consequently Eq.32 becomes

$$R(M_{SUSY}) = \frac{R^*_{MSSM}}{1 + \Delta'_{MSSM} [x' - 1]} \qquad (36)$$

where x' given by

$$x' = x\Delta_X + \frac{R^*_{MSSM}}{R^*_X}(1 - \Delta_X) \qquad (37)$$

with,

$$x = \frac{R^*_{MSSM}}{R(M_X)}, \quad \Delta_X = \left(\frac{\alpha(M_I)}{\alpha(M_X)} \right)^{B_{3X}} \qquad (38)$$

The relevant fixed point quantities above are shown in Table 3. Note that $\Delta_X > \Delta'_{MSSM}$ (except in model K) where the values are comparable to Δ_{GUT} given for various models with no extra families in ref.[14]. This is not surprising or even significant since Δ'_{MSSM} is calculated using a much larger ratio of scales than Δ_X. The fact that $\Delta_X \ll 1$ is the important fact, and also that $\frac{R^*_{MSSM}}{R^*_X} < 1$, which implies that x' in Eq.37 is likely to be small.

In the case of SUSY GUTs, small values of x' imply that the MSSM QFP will be realised. Here we cannot exactly make this statement because the MSSM is now effective below the scale M_I, so the MSSM QFP here is not the same as the usual one. In order to overcome this difficulty we combine Eqs.36 and 37 into a single equation which yields the low energy top quark Yukawa coupling directly from the string scale boundary conditions,

$$R(M_{SUSY}) = \frac{R^*_{MSSM}}{1 + \Delta'_{MSSM} \left[\left(x\Delta_X + \frac{R^*_{MSSM}}{R^*_X}(1 - \Delta_X) \right) - 1 \right]} \qquad (39)$$

19

Model	R_X^*	B_{3X}	$\frac{R_{MSSM}^*}{R_X^*}$	Δ'_{MSSM}	Δ_X
A	5/9	-5/3	7/10	0.56	0.80
B	13/18	-13/3	7/13	0.52	0.87
C	13/18	-13/3	7/13	0.56	0.73
D	19/18	19/3	7/19	0.57	0.60
E	8/9	*	7/16	0.51	0.89
F	8/9	*	7/16	0.52	0.78
G	11/9	11/3	7/22	0.52	0.78
H	19/18	19/3	7/19	0.50	0.90
I	11/9	11/3	7/22	0.57	0.54
J	8/9	*	7/16	0.56	0.67
K	14/9	7/3	1/2	0.57	0.39
L	19/18	19/3	7/19	0.51	0.87
M	25/18	25/9	7/25	0.51	0.83
N	11/9	11/3	7/22	0.50	0.91
X	43/18	43/27	7/43	0.50	0.78

Table 3: Fixed point properties as discussed in the text of the MSSM+X models defined in Table 1. Δ'_{MSSM} and Δ_X are relevant for $\alpha_S(M_Z) = 0.117$, $M_{SUSY} = 500$ GeV and $m_t^{phys} = 174$ GeV.

It is clear from Eq.39 that a low energy QFP will be achieved when the following condition is met:

$$x\Delta_X \ll 1 \tag{40}$$

which should be compared to the MSSM QFP condition $x' \ll 1$. Since in general $\Delta_X < 1$, Eq.40 shows that in MSSM+X models the QFP condition is more easily achieved than in the MSSM. The effect is greater for the MSSM+X models with the smaller values of Δ_X in Table 3.

When the condition in Eq.40 is satisfied, the low energy top Yukawa coupling is given approximately independently of its string scale input value. In other words there is a QFP given by

$$R(M_{SUSY}) \approx \frac{R_{MSSM}^*}{1 - \Delta} \tag{41}$$

where

$$\Delta = \Delta'_{MSSM}\left[1 - \frac{R_{MSSM}^*}{R_X^*}(1 - \Delta_X)\right] \tag{42}$$

where we have written Eq.39 in the form of Eq.23, and have made the approximation in Eq.40.[6]

---

[6]For the case where the intermediate effective theory has a zero QCD beta function, a similar expression is found although we do not go into detail here.

$\alpha_3(M_Z)$	M_{SUSY}/GeV	Δ
0.112	200	0.46
0.112	1000	0.51
0.122	200	0.44
0.122	1000	0.50

Table 4: The quantity Δ for the MSSM and the models A,...,N,X.

The values of Δ in Eq.42 were determined for each of these models and were found to within the accuracy of our calculations to be independent upon which particular MSSM+X model was used. In other words we find $\Delta \approx \Delta_{MSSM}$ for all of the MSSM+X models. This seems at first sight to be somewhat surprising since Δ depends on Δ'_{MSSM}, R^*_X and Δ_X, all of which vary from model to model. Somehow all these quantities conspire to give $\Delta \approx \Delta_{MSSM}$. The explanation is simply that the lower energy dynamics (below M_I) has the most important focusing effect on the large top Yukawa coupling and all the higher energy differences become irrelevant. Thus the high energy structure of the MSSM+X models above the intermediate scale makes little difference to the QFP prediction. Of course the high energy structure of the MSSM+X models is vital in determining whether the top Yukawa coupling is in the QFP region at all, as is clear from Eq.40. Also it is clear that the value of Δ_{MSSM} and hence Δ is sensitive to the input parameters ($\alpha_3(M_Z)$ and M_{SUSY}) as shown in Table 4. The dependence of Δ upon m_t was found to be negligible.

The above analytic results take into account only the QCD coupling. If electroweak corrections to Eq.20 are applied [22], there is no longer an exact fixed point and the approximate quasi-fixed-point value of $m_t^{phys}/\sin\beta$ increases from ~ 180 GeV to ~ 200 GeV[7] where m_t^{phys} refers to the physical (pole) mass of the top quark. Thus these additional corrections are quite important and must be considered. In Figs.10,11,12 we display the full numerical predictions for the MSSM+X and MSSM models, obtained by numerically integrating the RG equations including all the Higgs and electroweak couplings in addition to the QCD coupling[8]. The MSSM* curve corresponds to the MSSM particle content and gauge group up to $\mu = 4 \times 10^{17}$ GeV, and is intended to show the added focusing effect of increasing the range of μ by a factor of 20 compared to the MSSM. The top quark mass (scaled by $\sin\beta$) is plotted as a function of the input variable $x = \frac{R^*_{MSSM}}{R(M_X)}$. Since x is proportional to $1/Y_t(M_X)$, the zero intercept on the horizontal axis corresponds to the quasi-fixed-points of the models. Note that the scale M_X at which the input couplings $\frac{1}{R(M_X)} = \frac{\tilde{\alpha}_3(0)}{Y_t(0)}$ are defined differs from curve to curve. The MSSM (MSSM*)has its input couplings defined at 10^{16}GeV (4×10^{17} GeV), while the other models have M_X in the range $3.5 - 5.5 \times 10^{17}$ GeV,

---

[7]This number is quite dependent on the input parameters. For example, if $M_{SUSY} = 2$ TeV, the quasi-fixed-point corresponds to $m_t^{phys}/sin\beta \sim 220$ GeV.

[8]For $M_{SUSY} = 1$ TeV, $\alpha(M_X) = 1/24$, $M_X = 1.2 \times 10^{16}$ GeV, the MSSM curve agrees with the plot in ref.[14]
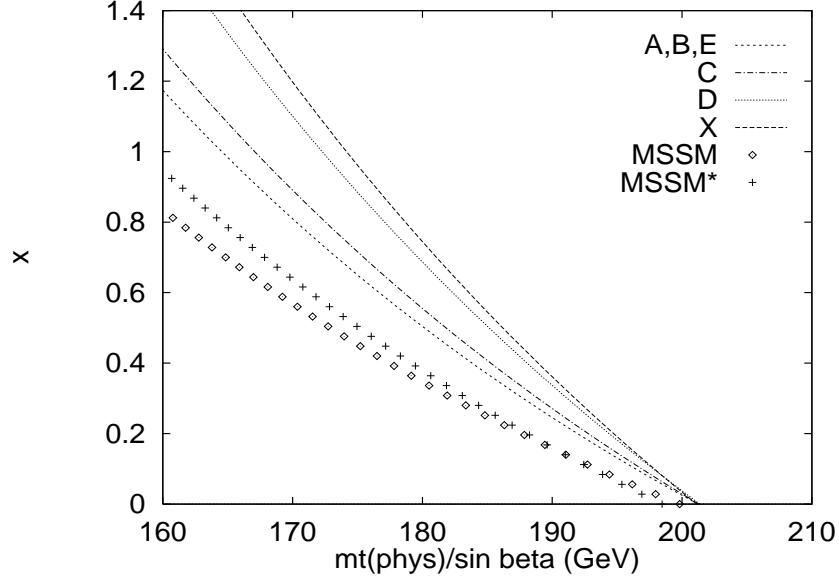
Figure 10: $m_t^{phys}/\sin\beta$ as a function of the variable $x = \frac{R^*_{MSSM}}{R(M_X)}$ for MSSM+X models A,B,C,D,E,X and the MSSM for $M_{SUSY} = 500\,\text{GeV}$, $\alpha_3(M_Z) = 0.117$. The unification scale $t = 0$ for the MSSM (MSSM*) is assumed to be $M_{GUT} = 10^{16}(4.10^{17})\,\text{GeV}$.

as shown in Fig.1. Varying $M_{SUSY} = 200 - 1000$ GeV and $\alpha_3(M_Z) = 0.112 - 0.122$ produces a maximum (but significant) 5% error in $m_t^{phys}/\sin\beta$.

The models in Figs.10,11,12 corresponding to the steepest graphs correspond to the MSSM QFP prediction of the top quark Yukawa coupling being more likely to be realised (a vertical line would predict the top quark mass independently of the input Yukawa coupling.) These results may be compared to the MSSM results which are also plotted, where in this case we have assumed the high energy scale to be M_{GUT} so that $x = x'$ in this case. All the MSSM+X models are steeper than the MSSM line, indicating the increased likelihood that the QFP is realised. The amount of the effect which is due to the extra factor of ~ 20 in the range of running is illustrated by the MSSM* curve where a higher energy scale comparable to the string scale is assumed to be M_{GUT}. The graphs with the highest number of $SU(2)_L$ doublets (i.e. high p) are the steepest. This is in part due, however, to the fact that many of these models have higher $\alpha_3(0) = \alpha_X = \alpha(M_X)$, as is clear from Fig.7. These plots make the focusing effect of the fixed point clear: for example, model K predicts $m_t^{phys}/\sin\beta > 185$ GeV for $x < 1$. These numerical results support the earlier analytical expectations that the smaller the value of Δ_X, the closer a particular model is likely to be to the QFP.
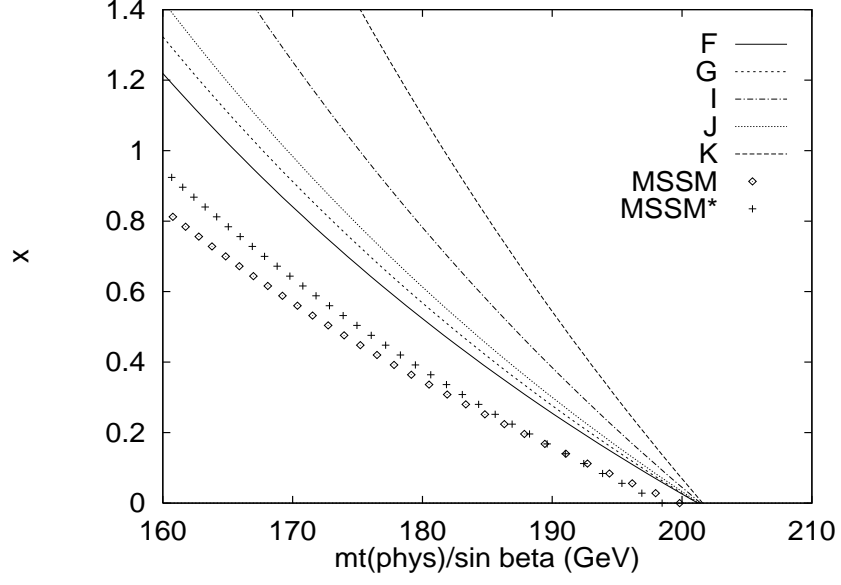
Figure 11: $m_t^{phys}/\sin\beta$ as a function of the variable $x = \frac{R^*_{MSSM}}{R(M_X)}$ for MSSM+X models F,G,I,J,K and the MSSM for $M_{SUSY} = 500$ GeV, $\alpha_3(M_Z) = 0.117$. The unification scale $t = 0$ for the MSSM (MSSM*) is assumed to be $M_{GUT} = 10^{16}(4.10^{17})$ GeV.
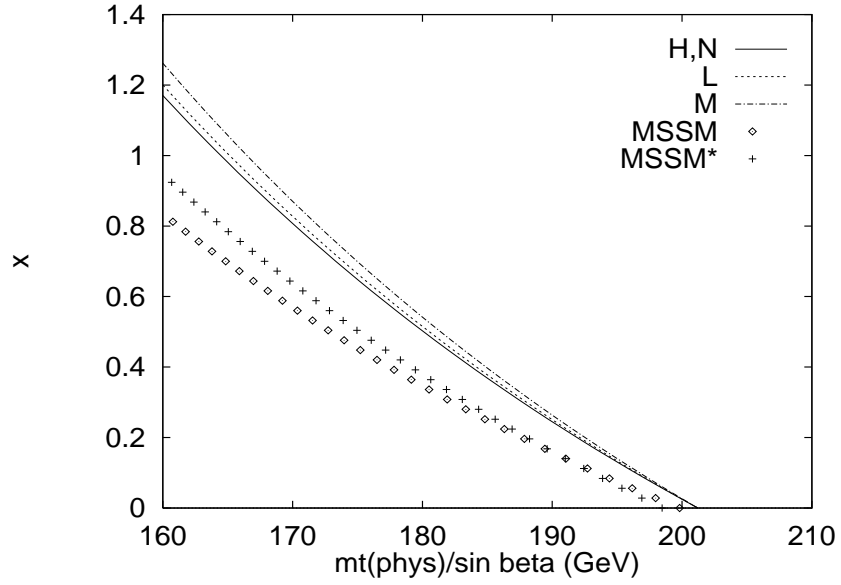

Figure 12: $m_t^{phys}/\sin\beta$ as a function of the variable $x = \frac{R^*_{MSSM}}{R(M_X)}$ for the MSSM+X models H,L,M,N and the MSSM for $M_{SUSY} = 500$ GeV, $\alpha_3(M_Z) = 0.117$. The unification scale corresponding to $t = 0$ for the MSSM (MSSM*) is assumed to be $M_{GUT} = 10^{16}(4.10^{17})$ GeV.

4 Origin of Yukawa Matrices with Texture Zeroes in MSSM+X Models

So far we have been concerned with the issues of gauge coupling unification, and the determination of the top quark Yukawa coupling via the infra-red fixed point structure of the MSSM+X models. We have seen that the physical top quark mass is determined to some extent by the infra-red fixed point of the theory, and so the next obvious question is to what extent the remainder of the Yukawa matrices may be determined. We leave the highly model-dependent possibility that the lighter fermion masses are generated at the level of string theory alone and instead concentrate on a possible mechanism at the effective field theory level.

Some time ago, Ibanez and Ross [15] showed how the introduction of a gauged $U(1)_X$ family symmetry could be used to provide an explanation of successful quark and lepton Yukawa textures within the framework of the MSSM. The idea is that the $U(1)_X$ family symmetry only allows the third family to receive a renormalisable Yukawa coupling but when the family symmetry is broken at a scale not far below the string scale other families receive suppressed effective Yukawa couplings. The suppression factors are essentially powers of the VEVs of θ fields which are MSSM singlets but carry $U(1)_X$ charges and are responsible for breaking the family symmetry. These Yukawa couplings are scaled by heavier mass scales M identified as the masses of new heavy vector representations which also carry $U(1)_X$ charges. For example, one may envisage a series of heavy Higgs doublets of mass M with differing $U(1)_X$ charges which couple to the lighter families via sizable Yukawa couplings which respect the family symmetry. The heavy Higgs doublets also couple to the MSSM Higgs doublets via θ fields and this results in suppressed effective Yukawa couplings when the family symmetry is broken. For more details of this mechanism see ref.[15].

Recently Ross [16] has combined the idea of a gauged $U(1)_X$ family symmetry with the previous discussion of infra-red fixed points. The idea behind this approach is that since there are no small Yukawa couplings one may hope to determine all the Yukawa couplings by the use of infra-red fixed points along similar lines to the top quark Yukawa coupling determination. An explicit model was discussed in detail [16]. The explicit model was based on the MSSM gauge group persisting right up to the string scale. The question of gauge coupling unification was addressed [16] by adding complete $SU(5)$ vector representations to the MSSM theory with masses just below the unification scale. These have no relative effect on the running of the three gauge couplings to one loop order, however at two loop order it was claimed that the unification scale is raised. By adding a sufficiently large number of such states it was hoped that the unification scale could be postponed to the string scale by a combination of two loop gauge running and threshold effects, although this mechanism was not studied in detail in ref.[16]. This mechanism is obviously quite different to the one loop approach to gauge unification within the MSSM+X models considered here, and it is clearly of interest to see if the $U(1)_X$ family symmetry approach can be accommodated within this class models.
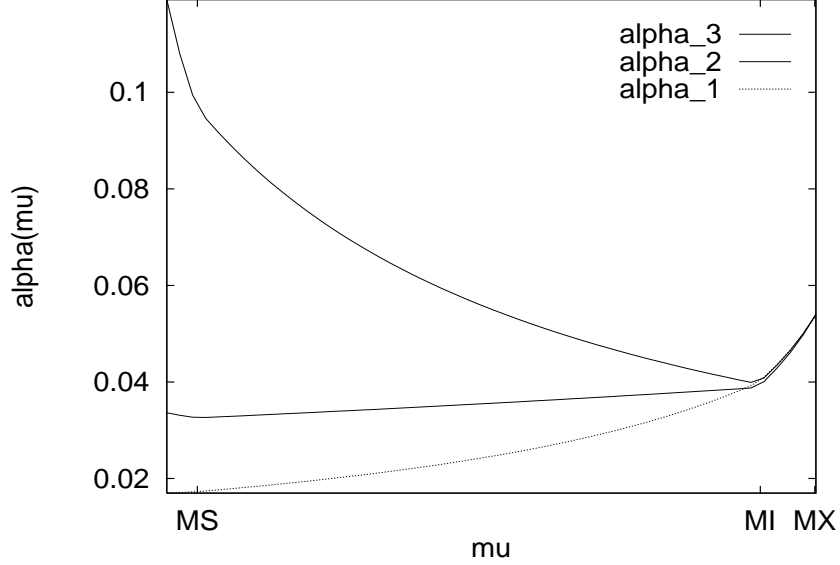
Figure 13: The running of the three Standard Model gauge couplings in model X between $\mu = M_Z$ and $\mu = M_X$ for $\alpha_S(M_Z) = 0.1192$, $M_{SUSY} = 500$ GeV, $m_t^{phys} = 174$ GeV. The normalisation $k_1 = 5/3$ for the hypercharge gauge coupling has been used.

In order to obtain the desired Yukawa textures it is necessary to add several heavy Higgs doublets in vector representations and with various $U(1)_X$ charges in addition to the two Higgs doublets of the MSSM [15, 16]. In ref.[16] each of these Higgs representations is accompanied by a colour triplet in order to make up a complete $SU(5)$ representation, where such triplets are forbidden from mixing with quarks by R-symmetry. From our point of view, in MSSM+X models there is necessarily additional matter at the intermediate scale M_I which has to be present in order to satisfy the condition of one loop gauge coupling unification which we have imposed on the models. Many of the models involve additional doublets which may be identified with Higgs doublets if they have suitable hypercharges, and so it is natural for us to put this extra matter to work for us in providing the Yukawa structures. In principle there is no restriction on the magnitude of the intermediate scale M_I, corresponding to the masses of the extra Higgs doublets, since it may be assumed that the $U(1)_X$ family symmetry is broken slightly below this scale yielding phenomenologically acceptable suppression ratios in the effective Yukawa couplings of $< \theta > /M_I \sim 0.2$. However there is a technical restriction that the $U(1)_X$ family symmetry should not be broken more than a couple of orders of magnitude below the string scale since its anomaly freedom relies on the Green-Schwarz mechanism [15]. In fact, the Green-Schwarz mechanism requires

$$\frac{\langle \theta \rangle}{M_X} \sim O(\frac{1}{\sqrt{192}\pi}), \tag{43}$$

and since $\langle \theta \rangle/M_I \sim 0.2$, we must have $M_I/M_X \sim O(1/8)$ for the mechanism to work.

Let us consider as an example the model discussed in ref.[16] in which the Higgs doublets of the MSSM may be written as $H_1^{(0)}, H_2^{(0)}$, and the extra Higgs doublets may be written as:[9]

$$H_{1,2}^{-1}, \bar{H}_{1,2}^{1}, H_{1,2}^{-2}, \bar{H}_{1,2}^{2}, H_{1,2}^{3}, \bar{H}_{1,2}^{-3}, H_{1,2}^{4}, \bar{H}_{1,2}^{-4}, H_{1,2}^{8}, \bar{H}_{1,2}^{-8}, \tag{44}$$

where the $U(1)_X$ charges are given in parentheses, and $H_{1,2}^{(x)}$ have hypercharges $Y/2 = -1/2, 1/2$, and $\bar{H}_{1,2}^{(-x)}$ have hypercharges $Y/2 = 1/2, -1/2$, respectively. The idea is that the Higgs $H_{1,2}^{(x)}$ have direct couplings to the lighter families and mix with the MSSM Higgs $H_{1,2}^{(0)}$ via singlet θ fields, thereby generating hierarchical Yukawa structures. If the extra Higgs doublets are interpreted as intermediate scale matter then this corresponds to $b = 10$, where b labels the number of additional vector (1,2) representations. This model may be embedded in model X which was considered previously, and chosen with this discussion in mind. In Model X, M_I is not too far below M_X; choosing for example $\alpha_S(M_Z) = 0.1192$, we have $M_I/M_X \sim 1/25$. If we assume that all the other additional superfields have zero hypercharge assignment, then we determine $k_1 = 5/3$, just right for the Green-Schwarz mechanism to work. These hypercharge assignments have the added advantage that they automatically ban any mass mixing terms (above $\mu \sim M_W$) between the ordinary quark fields and the heavy (3,1) or (3,2) fields. Fig.13 displays the running of the three gauge couplings for $\alpha_S(M_Z) = 0.1192$. It turns out that this model has $M_I = 1.7 \times 10^{16}$ GeV$\sim M_{GUT}$ and the intermediate matter performs the job of making the couplings run with similar slope above M_{GUT}.

Whereas the conditions upon M_I/M_X and k_1 implied by the Green-Schwarz mechanism are non-trivial to solve in the context of the gauge unified MSSM+X models and in general are only satisfied for some subspace of the phenomenologically allowed values of $\alpha_S(M_Z) = 0.112 - 0.122$ and M_{SUSY}, model X is only one example of a class of possible models. For example, by adding more doublets it is possible to increase M_I/M_X in order to reach 1/8. It may however, be possible to construct [23] models with less particle content than model X in which the matter is at slightly different scales, or in which the θ field is not added vectorially [24], in order to circumvent the possible problem of D-flatness [15]. Here we are only concerned with presenting a model of fermion masses that fits in with string-scale gauge unification.

5   Conclusion

We have taken the idea of intermediate scale matter to explain stringy gauge unification seriously within the context of Kac-Moody level 1 superstrings. To make our calculation not depend upon the precise string model chosen, we have made crude,

---

[9]In fact this model must necessarily involve yet more Higgs doublets in order to achieve Cabibbo mixing. However for illustrative purposes we shall only consider those Higgs doublets listed in ref.[16].

simplifying approximations. A strong approximation is the neglect of heavy or string threshold effects around M_X. Another source of these uncertainties could come from the assumption that the superpartner masses are all degenerate at M_{SUSY}. It is well known that a significant relaxation of this assumption may change the constraints of gauge unification[10]. One reason that we do not worry too much about these possible effects is that a previous analysis [9] showed that not only can these effects alone not explain the discrepancy in unification of the gauge couplings at the string scale, they sometimes tend to make the problem worse. Another approximation we have made [25] is that of the step function for particle thresholds. We do not expect this uncertainty to be significant in a one loop calculation.

One important question which we have hitherto left unanswered is: where does the extra matter come from and why does it have the mass $M_I \ll M_X$? There are several possible solutions to this question: it is possible that it is connected to some sort of hidden sector dynamics [18], possibly related to supersymmetry breaking. Another possibility is of some non-renormalisable operators coming straight from the string [9]. Models with high additional numbers of right handed quark fields have M_I about an order of magnitude below M_X and so the problem of how the $M_I - M_X$ hierarchy arises in these models may not be relevant.

We have systematically analysed what constraints there exist on the extra matter when it all has roughly an equivalent mass for up to 5 vector representations additional to the MSSM. Predictions for the scales M_I, M_X are given by the string gauge unification conditions. It is also found that the number of extra right handed quark type fields must exceed the number of the extra left handed quark and lepton (or Higgs) supermultiplets if the gauge couplings are to unify at the string scale. We emphasise again that, unlike the analysis in ref.[11], we have not imposed the GUT normalisation value of k_1 on the models, so the identification of the extra matter with exotic quarks and leptons or Higgs doublets is for descriptive purposes only since the hypercharge assignments are arbitrary. In fact we have obtained upper bounds on k_1 for each of the models under consideration. The theoretical lower bound of $k_1 > 1$ has also been used to place a restriction on the sum of the squared hypercharges of the additional matter for each of the models.

A large part of this paper has been concerned with the top quark Yukawa coupling fixed points in MSSM+X models. The effect of the additional matter above the intermediate scale is seen to make the MSSM QFP low energy prediction of the top quark mass more likely than in the MSSM, with the result that the physical top quark tends to be heavier. In this respect the MSSM+X models behave rather similarly to the SUSY GUT theories which contain a large number of representations [14]. We studied this effect both analytically, using the simple approximation of retaining only the QCD gauge coupling constant, and numerically keeping all three gauge couplings. The full numerical solutions for the top quark mass in the MSSM+X models are given in Figs.10,11,12. One way of summarising our results is to say that, once the MSSM is correctly adjusted in order to give string unification, the top quark mass is more

---

[10]And is likely to give flavour changing neutral current effects excluded by experiment.

likely to be determined by its MSSM QFP than in the standard MSSM. Of course the QFP prediction itself is the same in both the MSSM and the MSSM+X models; it is just that in the MSSM+X models the QFP prediction is more likely to realised.

The problem of the origin of the lighter fermion masses was also discussed briefly in the context of Abelian family gauge symmetries. An example is found, which we referred to as Model X, which is phenomenologically acceptable as a candidate for this scenario, having the properties that $k_1 = 5/3$ and an intermediate scale not too far below the string scale as shown in Fig.13. In Model X, ten of the extra vector representations are identified as extra Higgs doublets and are assigned the appropriate hypercharges. Following the scenario of refs.[15, 16], the gauged $U(1)_X$ family symmetry is assumed to be broken, leading to mixing of the standard and extra Higgs doublets, and resulting in small effective Yukawa couplings and approximate texture zeroes, once suitable family charges are assumed. There are undoubtedly more examples of a similar nature in addition to Model X [23]. Needless to say, in common with the other MSSM+X models, Model X also favours the MSSM QFP prediction of the top quark mass.

To conclude, we find the fusion of the MSSM+X approach to gauge coupling unification and the $U(1)_X$ gauged family symmetry and infra-red fixed point approach to fermion masses to be a very promising and exciting area which deserves further study.

References

[1] U.Amaldi et al., Phys. Rev. **D36** (1987) 1385;
    P.Langacker and M.Luo, Phys. Rev. **D44** (1991) 817;
    J.Ellis,S.Kelley and D.V.Nanopoulos, Phys. Lett. **B249** (1990) 441;
    Nucl. Phys. **B373** (1992) 55;
    U.Amaldi, W. de Boer and H.Fustenau, Phys. Lett. **B260** (1991) 447;
    C. Giunti, C.W. Kim and U.W. Lee, Mod. Phys. Lett. **A6** (1991) 1745;
    H.Arason et al., Phys. Rev. **D46** (1992) 3945;
    F.Anselmo, L.Cifarelli, A.Peterman and A.Zichichi, Nuovo Cimento 105A (1992) 1179;
    P.Langacker and N.Polonski, Phys. Rev. **D47** (1993) 4028;
    A.E.Faraggi and B.Grinstein, Nucl. Phys. **B422** (1994) 3.

[2] L. Hall and S. Raby, Phys. Rev. **D51** (1995) 6524.

[3] J.Ellis, S. Kelley and D.V.Nanopoulos, Phys. Lett. **B249** (1990) 241;
    C.Bachas, C.Fabre and T.Yanagida, NSF-ITP-95-129, CPTH-S379.1095, hep-th/951004;
    P.H.Chankowski, Z.Pluciennik, S. Pokorski and C.E.Vayonakis, Phys. Lett. **B358** (1995) 264;

A. de la Macorra, Phys. Lett. **B341** (1994) 31;
H.P.Nilles, TUM-HEP-234/96, SFB-375/28.

[4] V.Kaplunovsky, Nucl. Phys. **B307** (1988) 145.

[5] C.Bachas and C.Fabre, hep-ph/9505318;
A.A.Maslikov, I.A.Naumov and G.G.Volkov, hep-ph/9512429.

[6] D. Lewellen, Nucl. Phys. **B337** (1990) 61;
A. Font, L. Ibanez and F. Quevedo, Nucl. Phys. **B345** (1990) 389;
S. Chaudhuri, S-w Chung and J. Lykken, hep-ph/9405374;
G.Aldazabal, A.Font, L.E.Ibanez and A.M.Uranga, Nucl. Phys. **B452** (1995) 3;
I.A.Antionadis, J.Ellis, J.Hagelin and D.V.Nanopoulos, Phys. Lett. **B194** (1987) 231;
I.A.Antionadis, J.Ellis, J.Hagelin and D.V.Nanopoulos, Phys. Lett. **B231** (1989) 65;
I.A.Antionadis and G.K.Leontaris, Phys. Lett. **B216** (1989) 33;
I.A.Antionadis, G.K.Leontaris and J.Rizos, Phys. Lett. **B245** (1990) 161.

[7] L.E.Ibanez, Phys. Lett. **B318** (1993) 73.

[8] Choi and Kiwoon, Phys. Rev. **D37** (1988) 1564;
P. Mayr, H.P.Nilles and S.Steinberger, Phys. Lett, **B317** (1993) 53;
D.Bailin and A.Love, Phys. Lett. **B292** (1992) 315;
E. Halyo, hep-ph/9509323;
V.Kaplunovsky, Nucl. Phys. **B307** (1988) 145;
I.A.Antionadis, J.Ellis, R.Lacaze and D.V.Nanopoulos, Phys. Lett. **B268** (1991) 188;
J.P.Deredinger, S.Ferrara, C.Kounnas and F.Zwirner, Phys. Lett. **B271** (1991) 307;
J.P.Deredinger, S.Ferrara, C.Kounnas and F.Zwirner, Nucl. Phys. **B372** (1992) 145;
L.Ibanez, D.Lust and G.G.Ross, Phys. Lett. **B272** (1991) 251;
L.Dixon, V.Kaplunovsky and J.Louis, Nucl. Phys. **B335** (1991) 649;
I.A.Antionadis, E.Gava, K.S.Narain and T.Taylor, Nucl. Phys. **B407** (1993) 706;
E.Kiritsis and C.Kounnass, Nucl. Phys. **B442** (1995) 472;
V.Kaplunovsky and J.Louis, Nucl. Phys. **B444** (1995) 191;
P.M.Petropoulos and J.Rizos, hep-th/9601037.

[9] K.R.Dienes and A.E.Faraggi, Phys. Rev. Lett. **75** (1995) 2646;
K.R.Dienes and A.E.Faraggi, Nucl. Phys. **B457** (1995) 409.

[10] J.Ellis, S.Kelley and D.V.Nanopoulos, Phys. Lett. **B260** (1991) 131;
I. Antoniadis, J. Ellis, S. Kelley and D.V. Nanopoulos, Phys. Lett. **B272** (1991) 31;
D.Bailin and A.Love, Phys. Lett. **B280** (1992) 26;
D.Bailin and A.Love, Mod. Phys. Lett. **A7** (1992) 1485;

J.Lopez and D.V.Nanopoulos, DOE-ER-40717-20, CTP-TAMU-45-95, ACT-16-95, hep-ph/9511426;
A.E.Faraggi, Phys. Lett. **B302** (1993) 202;
J.Lopez, D.V.Nanopoulos and K.Yuan, Nucl. Phys. **B335** (1990) 347;
M.K.Gaillard and R.Xiu, Phys. Lett. **B296** (1992) 71;
I.A.Antionadis and K.Benakli, Phys. Lett. **B295** (1992) 219;
R.Xiu, Phys. Rev. **D49** (1994) 6656.

[11] S.Martin and P.Ramond, Phys. Rev. **D51** (1995) 6515.

[12] B.Pendleton and G.Ross, Phys. Lett.**B98** (1981) 291.

[13] C.Hill, Phys. Rev. **D24** (1981) 691.

[14] M.Lanzagorta and G. Ross, Phys. Lett. **B349** (1995) 319.

[15] L.Ibanez and G.Ross, Phys. Lett. **B332** (1994) 100.

[16] G.G.Ross, Phys. Lett. **B364** (1995) 216.

[17] A.E.Faraggi, Phys. Rev. **D46** (1992) 3204.

[18] J.L.Lopez and D.V.Nanopoulos, CTP-TAMU-41/95, DOE/ER/40717 19, ACT-15/95, hep-ph/9511266;
G.K.Leontaris and N.D.Tracas, IOA 327/95, NTUA 53/95, hep-ph/9511280;
G.K.Leontaris, Phys. Lett. **B281** (1992) 54;
R.Barbieri, G.Dvali and A.Strumia, Phys. Lett. **B33** (1994) 79;
J.L.Lopez, D.V.Nanopoulos and A.Zichichi, CTP-TAMU-01/96, DOE/ER/40717-24, ACT-01/96, hep-ph/9601261.

[19] K.Dienes, A.Faraggi and J.March-Russell, hep-th/9510223.

[20] CDF collaboration, Phys. Rev. Lett. **73**, (1994) 225.

[21] A.E.Faraggi, hep-ph/9506388.

[22] V.Barger, M.S.Berger and P.Ohmann, Phys. Rev. **D47** (1993) 1093.

[23] B.C.Allanach and S.F.King, work in progress.

[24] P.Bientruy, S.Lavignac and P.Ramond, LPTHE-ORSAY 95/54, UFIFT-HEP-96-1,hep-ph/9601243.

[25] L.Clavelli and P.W.Coulter, UAHEP-954, hep-ph/9507261.